Chapter 4
Space-Domain Fiber Cavity Ring-Down Magnetic Field Sensor Using D-shaped Fiber Coated with Magnetic Fluid

Wenjia Chen, Chunfu Cheng, Jiaxuan Chen, Yiwen Ou, Li Fang, and Mengmeng Li

Abstract A space-domain fiber cavity ring-down magnetic field sensor is proposed and experimentally demonstrated. The enhanced evanescent field effect and stability was achieved by using D-shaped fiber coated with magnetic fluid as the sensor head, and a temperature controller was introduced to improve the measurement accuracy. With this novel technique, magnetic field sensing has been demonstrated by measuring ring-down distance and a sensitivity of 8.4×10^{-4} dB/Gs in the linear region was achieved.

4.1 Introduction

Time-domain fiber cavity ring-down (FCRD) technique has attracted much attention recently due to its high sensitivity [1]. In this scheme, through measuring the ring-down time [2], the loss induced by the tested sample can be deduced. As this technique does not measure the absolute intensity of light source, it is insensitive to light intensity fluctuations of the light source [3]. In addition, it has the advantages of high sensitivity due to multiple effective interactions with the sample; therefore, it was utilized by many researchers to monitor different parameters. Combined with different sensor heads, different parameters including refractive index of liquids [4–6], macro-bend loss of single-mode fiber (SMF) have been measured using this scheme [7]. However, the traditional time-domain FCRD technique uses expensive equipment, such as pulsed light sources, pulse modulators, fast detectors, and high-speed oscilloscopes, to observe ring-down signals in time-domain, thus resulting in high costs. Ye and Qian et al. [8], based on frequency-shifted interferometry (FSI), propose a new FCRD technique which adopts continuous light, low-speed differential detector and a low-speed, low-cost acquisition card device to reduce instrument

W. Chen · C. Cheng (✉) · J. Chen · Y. Ou · L. Fang · M. Li
Hubei Engineering Technology Research Center of Energy Photoelectric Device and System,
Hubei University of Technology, Wuhan 430068, China
e-mail: chengchunfu@hbut.edu.cn

School of Science, Hubei University of Technology, Wuhan 430068, China

cost. In this technique, through Fast Fourier transform (FFT), a ring-down curve in the space domain can be obtained. Therefore, this new scheme can be called space-domain FCRD sensing technique. Compared with traditional time-domain FCRD technique, Space-domain FCRD crucially reduces technical costs while maintaining its original advantages, and the employed differential detection method can effectively eliminate DC noise which can increase signal-to-noise ratio and thus improving the system stability. Due to the excellent characteristics of space-domain FCRD, it has attracted wide attention from researchers and has been successfully applied to gas sensing [9], pressure sensing, [10] and stress sensing [11]. The magnetic field sensing plays an important role in a wide range of areas. Combining space-domain FCRD and D-shaped fiber to acquire highly sensitive optical fiber magnetic field sensor with high stability is of great significance and has vast application prospects.

In the paper, we propose and demonstrate a magnetic field sensor based on space-domain FCRD technique, and design a sensor head using D-shaped fiber coated with magnetic fluid. The technical principle and manufacturing method of the sensor head were demonstrated and the magnetic field has been monitored by measuring the ring-down distance. The experimental results have proved that a highly sensitive magnetic field sensor can be realized by using space-domain FCRD technique combined with D-shaped fiber.

4.2 Operation Principle and Experimental Setup

The proposed highly sensitive magnetic field sensing experimental setup based on space-domain FCRD is shown in Fig. 4.1. It is essentially composed of a ring-down cavity embedded in a Sagnac loop. An acousto-optic modulator is inserted
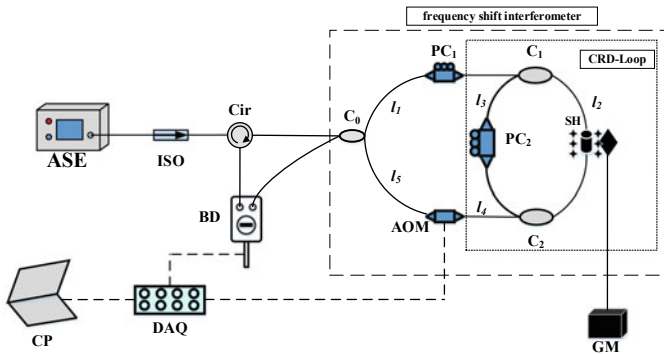
Fig. 4.1 Magnetic field sensing experimental setup based on space-domain FCRD technology. ASE: amplified spontaneous emission source; ISO: isolator; Cir: circulator; C_1:3 dB fiber coupler; C_2 and C_3: 99.5/0.5 fiber couplers; PC_1 and PC_2: polarization controller; SH: sensor head; AOM: acousto-optic modulator; BD: balanced detector; DAQ: data acquisition card; CP: Computer; GM: gaussmeter

asymmetrically in the Sagnac loop as a frequency shifter to form a frequency-shifted Sagnac interferometer. The principle of the frequency-shifted Sagnac interferometer is detailly explained in [12]. ASE emits continuous light of a frequency v and enters the Sagnac loop through the fiber coupler C_0, and thus it is divided into two light beams, one clockwise and another counterclockwise. The clockwise light directly enters the ring-down cavity, and the light leaks out of the ring-down cavity from the fiber coupler C_2 in each propagation and returns to the fiber coupler C_0 through the frequency shifter AOM. Meanwhile, the counterclockwise light firstly passes the frequency shifter AOM, then enters the ring-down cavity, next leaks out of the ring-down cavity through the fiber coupler C_1, and eventually returns to the fiber coupler C_0. The two light beams have the same frequency and a phase difference. When the coherence length of the light source is less than the ring-down cavity length d, the two light beams will interfere at the fiber coupler C_0. The differential interference signal detected by the balanced detector can be expressed as

$$\Delta I \infty \sum_{m=0}^{\infty} I_m \cos[2\pi \frac{n(mL + L_0)}{c} f] = \sum_{m=0}^{\infty} I_m \cos(2\pi F_m f) \qquad (4.1)$$

where I_m is the light intensity after the light propagates m times in the ring-down cavity, n is the effective refractive index of the single-mode fiber, L_0 is the length of the ring-down cavity, $L = l_1 + l_2 + l_4 - l_5$ is a constant, c is the speed of light, f is the frequency shift produced by the acousto-optic modulator, $F_m = n(mL + L_0)/c$ is the oscillation frequency. F_m is unique for each round-trip number m and is equally spaced by nd/c. Due to the inherent loss of the optical device in the cavity, the light intensity decays exponentially in the following relationship. It can be expressed as

$$I_m = I_0 \exp(-m\alpha_c/4.34) = I_0 \exp(-\frac{l}{4.34L}\alpha_c) \qquad (4.2)$$

where I_0 is the initial light intensity, $l = mL$ is the propagation distance of light in the ring-down cavity, and α_c is the inherent loss in the cavity. In traditional time-domain FLRD technique, the time that it takes for the light intensity to decay to 1/e of the initial light intensity is called the ring-down time. Correspondingly, in the space-domain FCRD technique, the distance of the light intensity attenuation to 1/e of the initial light intensity is called the ring-down distance. It can be expressed as

$$d_0 = 4.34 \frac{L}{\alpha_c} \qquad (4.3)$$

When different magnetic field intensity is applied, the refractive index of the magnetic fluid will change, and the loss in the cavity will also change, thus resulting in an additional loss. The ring-down distance becomes

$$d = 4.34 \frac{L}{\alpha_c + \alpha_m} \qquad (4.4)$$

where $\alpha_m = \gamma C H l_s$, γ is the magnetic-field-induced absorption coefficient, C is the concentration of magnetic fluid, H is the magnetic field strength, l_s is the length of the D-shaped fiber coated with magnetic fluid. Based on (4.3) and (4.4), the additional loss α_m can be expressed as

$$\alpha_m = 4.34L\left(\frac{1}{d} - \frac{1}{d_0}\right) = kH \qquad (4.5)$$

For a given space-domain FCRD sensing system, the additional loss has a linear relationship with the magnetic field strength (H). The slop k represents the sensitivity of the sensor to the magnetic field.

4.3 Experimental Results and Discussion

Combining space-domain FCRD scheme with magnetic field sensor head, the magnetic intensity can be measured. For magnetic field sensing, the key is to make a highly sensitive sensor head. The schematic diagram of the proposed sensor head is shown in Fig. 4.2a. The sensor head is composed of a D-shaped fiber (NIR-SPF-W1550-2, Micro photons Technology Co.) and magnetic fluid (EMG Series Water-based Ferrofluid, EMG-603P, Ferrotec, USA) depicted in Fig. 4.2b, which is packed by plexiglass as shown in Fig. 4.2c. There are two small holes on the surface of the upper plexiglass to fill the magnetic fluid. When the optical fiber is completely soaked in the magnetic fluid and there is not any bubble in the groove, the small hole is sealed with paraffin. In order to avoid the influence of temperature on the performance of the sensor head, we place the sensor head on a temperature controller based on Peltier effect. Due to the special structure of the D-shaped fiber, a strong evanescent wave into the magnetic fluid was generated. It is worth mentioning that the excessively strong evanescent wave and the excessively high concentration ($C_0 = 18.7\%$) of the water-based magnetic fluid make the light greatly absorbed by the magnetic fluid and thus the cavity loss is too large. Therefore, we use deionized water to dilute the magnetic fluid to an appropriate concentration (C = 4.39%) for reducing the cavity loss.

In the experiment, we wrapped the copper wire around the iron core to generate the magnetic intensity which is controlled by changing the current load on the copper coils. A Peltier-effect-based temperature controller was used to keep temperature unchanged. For magnetic fluid, when the external magnetic field H increases, the effective permittivity of the magnetic fluid system will change, thus resulting in changes in the refractive index of the magnetic fluid, and also it is worth noting that when the external magnetic field intensity H reaches a certain threshold, the refractive index is basically saturated without any change because higher magnetic field intensity can agglomerate more magnetic nanoparticles(MNPs) to form more longer chains, leading to the constant change of RI of the magnetic fluid until it

(a)　　　　　　　　　　　　(b)

(c)
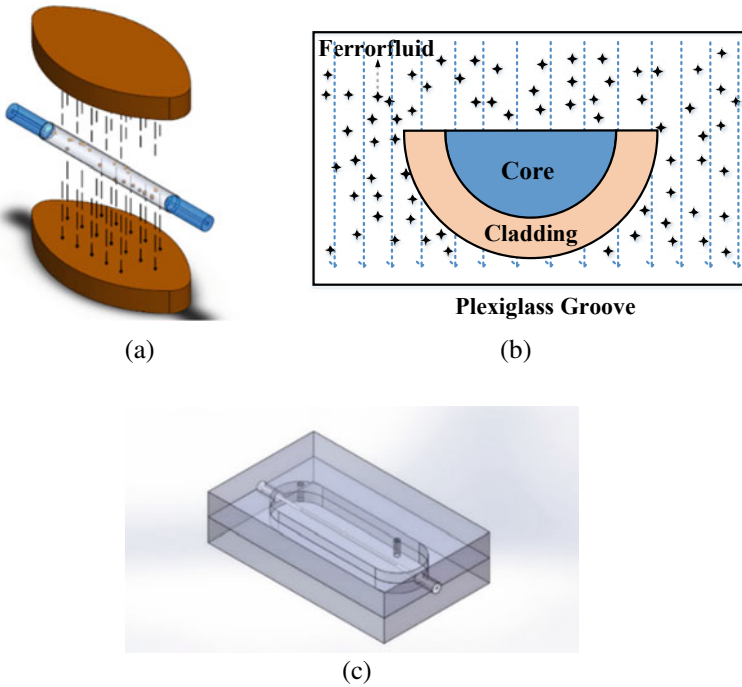
Fig. 4.2 **a** Schematic diagram of sensor head based on D-shaped fiber, **b** the cross section of the sensor head, **c** encapsulation of the sensor head

reaches saturation. When no external magnetic field was applied, the typical time-domain differential interference signal is collected by DAQ as shown in Fig. 4.3a. A series of ring-down signals in the space domain were obtained by performing FFT on the time-domain differential interference signal as shown in Fig. 4.3b. Then the peak value is extracted and fitted with an exponential function. The difference of the abscissas of the adjacent two peaks is 85.14 m (i.e., the cavity length) and the cavity loss is 1.138 dB, corresponding the ring-down distance which is 292.19 m according to (4.3).

Applying a magnetic field intensity of 0 Gs-400 Gs at increments of 50 Gs to the sensor head, we measure a series of ring-down signals in the space domain as shown in Fig. 4.4a and the corresponding exponential fit ring-down curves were shown in Fig. 4.4b. With the increase of the applied magnetic field intensity, the ring-down distance keeps decreasing,

which mainly resulted from the magnetic field deformations that occur as the magnetic field intensity varies [13]. To improve the measurement accuracy, the cavity loss under different magnetic field intensity is measured 30 times as shown in Figs. 4.4 and 4.5a. The increase of the magnetic field intensity leads to the increase of the ring-down cavity loss. On the other hand, it can be observed that when the magnetic field intensity is increased from 350 to 400 Gs, the cavity loss of the sensing
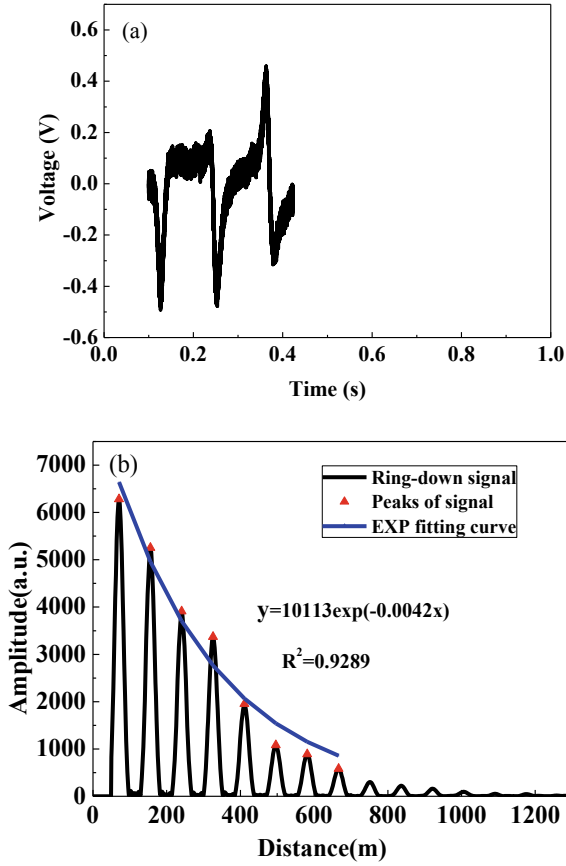
Fig. 4.3 **a** Detected ring-down signals, **b** Exponential fitted decay curve under 0–400 Gs magnetic field intensity
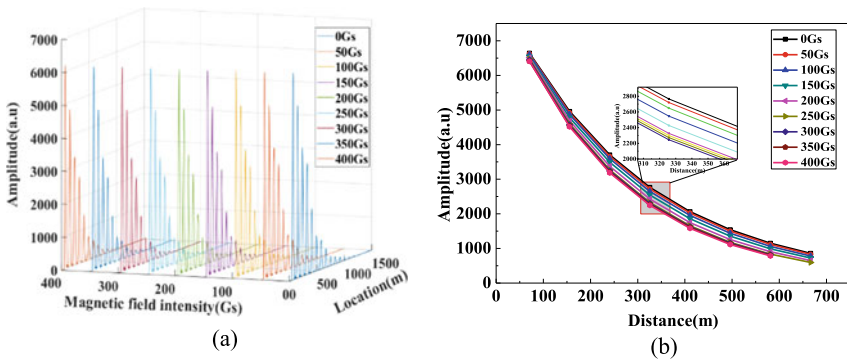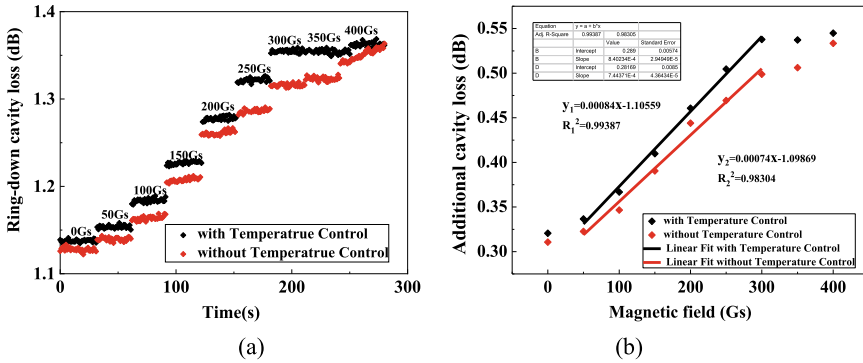

Fig. 4.4 **a** The Ring-down cavity loss responses to magnetic field applied on the sensor. **b** The relationship between the additional cavity loss and the magnetic field intensity

Fig. 4.5 Typical differential interference signal ΔI when the magnetic field intensity is 0 Gs. **a** the time-domain signal sampled by the DAQ; **b** the obtained space-domain FCRD signal after performing fast Fourier transform (FFT) on (**a**)

system is almost the same as that of the 300 Gs, thatis to say, the saturation effect of magnetic fluid occurs. MNPs determine the saturation magnetic field intensity of the magnetic fluid. When MNPs can no longer form longer and more chains under the impact of an external magnetic field, the magnetic field intensity at this time is regarded as the saturation magnetic field intensity. The saturation intensity of the magnetic fluid (EMG Series Water-based Ferrofluid, Ferrotec, USA) used in the experiment is 330 Gs, which is consistent with the experimental result. The basic carrier fluid of the magnetic fluid is usually deionized water or various oil-based magnetic field; therefore, the temperature has a significant impact on the magnetic field [14]. Figures 4.4 and 4.5a also shows the influence of magnetic field intensity on cavity loss with or without temperature control. Figures 4.4 and 4.5b illustrates the relationship between additional cavity loss and magnetic field intensity. Additional cavity loss linear increase with magnetic field intensity in range from 50 to 300 Gs, the R-square of 0.99 indicates that the sensing system have a good linear response, which agrees well with the theoretical result described in (4.5). The slope of the fitted straight line suggests that the measurement sensitivity is 8.4×10^{-4} dB/Gs. It also can be observed that sensitivity of sensor without temperature control is 7.4×10^{-4} dB/Gs which is lower than the sensitivity of sensor with temperature control. Therefore, the sensitivity is increased using the sensor head with temperature controller.

4.4   Conclusion

In conclusion, a novel magnetic sensing method based on space-domain FCRD is demonstrated. A highly sensitive sensor head is proposed by combining D-shaped fiber and magnetic fluid. By measuring the ring-down distance under different magnetic field intensities, the relationship between additional cavity loss

and magnetic field intensity can be obtained. The performance of the sensor in terms of sensitivity and linear response is experimentally studied. A sensitivity of 8.4×10^{-4} dB/Gs is obtained in the range of 50–300 Gs. The results indicate that the proposed sensor is low-cost, highly sensitive, and it exhibits the application potential for magnetic field detection in environment monitoring, aerospace, etc.

References

1. G. Berden, R. Engeln (eds.), Cavity ring-down spectroscopy: techniques and applications (2010)
2. F. Ye, C.M. Zhou, B. Qi, L. Qian, Continuous-wave cavity ring-down evanescent-field sensing with a broadband source based on frequency-shifted interferometry. Sensor Actuators B Chem. **184**, 150–155 (2013)
3. C. Wang, Fiber loop ringdown—a time-domain sensing technique for multi-function fiber optic sensor platforms: current status and design perspectives. Sensors **9**, 7595–7621 (2009)
4. N. Ni, C. Chan, L. Xia, P. Shum, Fiber cavity ring-down refractive index sensor. IEEE Photon. Technol. Lett. **20**, 1351–1353 (2008)
5. M. Jiang, W. Zhang, Q. Zhang, Y. Liu, B. Liu, Investigation on an evanescent wave fiber-optic absorption sensor based on fiber loop cavity ring-down spectroscopy, Opt. Commun. **283**, 249–253 (2010)
6. C. Wang, C. Herath, High-sensitivity fiber-loop ringdown evanescent-field index sensors using single-mode fiber. Opt. Lett. **35**, 1629–1631 (2010)
7. H. Berberoglu, H. Altan, A simple single-mode fiber loss measurement scheme in the C-band based on fiber loop-cavity ringdown spectroscopy. Opt. Commun. **317**, 29–33 (2014)
8. F. Ye, B. Qi, L. Qian, Continuous-wave fiber cavity ring-down measurements using frequency-shifted interferometry. Opt. Lett. **36**(11), 2080–2082 (2011)
9. C. Cheng, Z. Yang, Y. Ou, Z. Chen, J. Chen, H. Lv, Simultaneous measurement of gas composition and concentration combined fiber cavtiy ringdown and frequency-shifted interferometry. Optical Fiber Technol. **48**, 303–307 (2019)
10. Y. Ou, C. Cheng, Z. Chen, Z. Yang, H. Lv, L. Qian, Continuous-wave fiber cavity ringdown pressure sensing based on frequency-shifted interferometry. Sensors **18**(4), 1207 (2018)
11. C. Cheng, Z. Chen, Y. Ou, J. Chen, Multipoint fiber loop ringdown sensor for large strain measurement using frequency-shifted interferometry. Sensor **19** (13), 2907 (2019)
12. Y. Zhao, R. Lv, H. Li, Q. Wang, Simulation and experimental measurement of magnetic fluid transmission characteristics subjected to the magnetic field. IEEE Trans. Magn. **50**, 4600107 (2014)
13. E. Petrova, D. Kotsikau, V. Pankov, Structural characterization and magnetic properties of sol-gel derived $Zn_x Fe_{3-x}O_4$ nanoparticles. J. Magn. Magn. Mater. **378**, 429–435 (2015)
14. B. Sun, T. Shen, Y, Feng, Fiber-loop ring-down magnetic field and temperature sensing system based on the principle of time-division multiplexing. Optik **147**, 170–179 (2017)